Runoff characteristics and its sensitivity to climate factors in the Weihe River Basin from 2006 to 2018

WU Changxue[1], Xu Ruirui[2,3], QIU Dexun[2,3], DING Yingying[1], GAO Peng[1,2,3*], MU Xingmin[1,2,3*], ZHAO Guangju[1,2,3]

[1] State Key Laboratory of Soil Erosion and Dryland Farming on the Loess Plateau, Institute of Soil and Water Conservation, Northwest A&F University, Yangling 712100, China;
[2] State Key Laboratory of Soil Erosion and Dryland Farming on the Loess Plateau, Institute of Soil and Water Conservation, Chinese Academy of Sciences and Ministry of Water Resources, Yangling 712100, China;
[3] University of Chinese Academy of Sciences, Beijing 100000, China

Abstract: Exploring the current runoff characteristics after the large-scale implementation of the Grain for Green (GFG) project and investigating its sensitivities to potential drivers are crucial for water resource prediction and management. Based on the measured runoff data of 62 hydrological stations in the Weihe River Basin (WRB) from 2006 to 2018, we analyzed the temporal and spatial runoff characteristics in this study. Correlation analysis was used to investigate the relationships between different runoff indicators and climate-related factors. Additionally, an improved Budyko framework was applied to assess the sensitivities of annual runoff to precipitation, potential evaporation, and other factors. The results showed that the daily runoff flow duration curves (FDCs) of all selected hydrological stations fall in three narrow ranges, with the corresponding mean annual runoff spanning approximately 1.50 orders of magnitude, indicating that the runoff of different hydrological stations in the WRB varied greatly. The trend analysis of runoff under different exceedance frequencies showed that the runoff from the south bank of the Weihe River was more affluent and stable than that from the north bank. The runoff was unevenly distributed throughout the year, mainly in the flood season, accounting for more than 50.00% of the annual runoff. However, the trend of annual runoff change was not obvious in most areas. Correlation analysis showed that rare-frequency runoff events were more susceptible to climate factors. In this study, daily runoff under 10%–20% exceeding frequencies, consecutive maximum daily runoff, and low-runoff variability rate had strong correlations with precipitation, aridity index, and average runoff depth on rainy days. In comparison, daily runoff under 50%–99% exceeding frequencies, consecutive minimum daily runoff, and high-runoff variability rate had weak correlations with all selected impact factors. The sensitivity analysis results suggested that the sensitivity of annual runoff to precipitation was always higher than that to potential evaporation. The runoff about 87.10% of the selected hydrological stations were most sensitive to precipitation changes, and 12.90% were most sensitive to other factors. The spatial pattern of the sensitivity analysis indicated that in relatively humid southern areas, runoff was more sensitive to potential evaporation and other factors, and less sensitive to precipitation.

Keywords: daily runoff; climate-related factors; precipitation; potential evaporation; correlation analysis; sensitivity analysis; Weihe River Basin

Citation: WU Changxue, Xu Ruirui, QIU Dexun, DING Yingying, GAO Peng, MU Xingmin, ZHAO Guangju. 2022. Runoff characteristics and its sensitivity to climate factors in the Weihe River Basin from 2006 to 2018. Journal of Arid Land, 14(12): 1344–1350. https://doi.org/10.1007/s40333-022-0109-6

*Corresponding authors: GAO Peng (E-mail: gaopeng@ms.iswc.ac.cn); MU Xingmin (E-mail: xmmu@ms.iswc.ac.cn)
Received 2022-07-19; revised 2022-11-01; accepted 2022-11-08

1 Introduction

As an essential process of the hydrological cycle, the change in runoff plays a vital role in the sustainable development of human society, the economy, and the living environment (Greve et al., 2014; Sun et al., 2016). In the past few decades, the runoff of 24% of the world's major rivers has experienced significant changes, most notably declining trends in Asia's large rivers (Li et al., 2020). Yang et al. (2022) reported that from 1965 to 2018, the runoff of the Haihe River Basin, Liaohe River Basin, and Yellow River Basin in China showed a significant downward trend, leading to a sharp decline in the supply of ecosystem services and severe damage to human well-being. Therefore, it is of great significance to evaluate the influencing factors of runoff change for the development and utilization of water resources, agricultural production, and economic development (Sun et al., 2013).

In order to improve the ecological environment, a series of ecological environment protection measures have been taken in the basin (Ouyang et al., 2013). Among them, the Grain for Green (GFG) project has dramatically optimized the land use structure and improved ecosystem services (Zeng et al., 2020). The study of Yang et al. (2022) showed that abrupt changes in runoff in many rivers occurred in the 1990s, indicating that the implementation of the GFG project can reduce runoff. However, climate change also drives the hydrological cycle, primarily through changes in precipitation and temperature (Xie et al., 2015). Under global warming, hydrological variables such as surface runoff, evapotranspiration, and precipitation change greatly (Nilawar and Waikar, 2018). Therefore, studying the current runoff characteristics after the GFG project and investigating the runoff responses to climate-related factors will help us profoundly understand the water resource situation.

The Weihe River Basin (WRB) is a typical transition watershed of arid and semi-arid areas in China. Its water resources are susceptible to climate change (Song et al., 2007). Yang et al. (2014) found that climate factors could promote runoff in Northwest China. Qiu et al. (2022) found that the magnitude and frequency of extreme precipitation in the WRB have strengthened in the past 60 years and showed a strong aggregation mode. In addition, in some areas, higher potential evapotranspiration and temperature will also intensify the hydrological cycle (Li et al., 2016; Miao et al., 2016). As the largest primary tributary of the Yellow River Basin (YRB), the Weihe River not only provides a huge amount of water for the YRB and irrigates the Guanzhong Plain in the lower reaches of the Weihe River, but also maintains the ecological balance and social and economic development in Northwest China (Zuo et al., 2015). Since the large-scale implementation of the GFG project, runoff in the WRB has experienced a dramatic decreasing trend (Gao et al., 2013; Chang et al., 2015).

The relationships between runoff and climate factors are usually assessed by hydrological models or empirical statistical methods in the WRB. Gao et al. (2013) used the double-mass curves for the period 1932–2008 to quantify the contribution of precipitation to runoff change, and the results showed that the impact of precipitation on runoff decline accounted for only 17.20% before and after the transition year. Zhao et al. (2013) quantitively evaluated the impacts of climate change and human activities on runoff in the WRB from 1958 to 2008 based on Budyko curve method. They found that the decrease in annual runoff at most hydrological stations was due to the reduced precipitation and increased potential evaporation. Li et al. (2019) applied the Soil and Water Assessment Tool (SWAT) model in the WRB and found that in the tributaries and upstream hydrological stations, from 1970 to 2016, the dominant factor of runoff reduction was determined to be climate change, which accounted for more than 90.00%.

Previous studies have focused on the long-term change in runoff and its driving factors in the WRB while ignoring the current runoff characteristics. In addition, there are significant spatial differences in the geographical characteristics and climate types of the whole WRB, which makes the response of hydrological regimes in different places to climate change quite different (Huang et al., 2016). Existing studies primarily analyzed the sensitivity of the runoff at the outlet of the watershed to the potential influencing factors. However, they ignored the detailed and systematic

analysis of the relationship between climate variables (i.e., precipitation, evaporation, and other related parameters) and runoff characteristics of the whole WRB. In this study, several classical hydrological analysis methods were applied to analyze the runoff characteristics and its sensitivities to climate factors in the WRB from 2006 to 2018. The aims of this study are to (1) investigate the temporal and spatial variations in runoff characteristics of 62 hydrological stations in the WRB; (2) estimate the correlation between selected runoff characteristics and climate factors; and (3) calculate the sensitivities of annual runoff to precipitation, potential evaporation, and other factors based on an improved Budyko method.

2 Materials and methods

2.1 Study area

The WRB, located on the central Loess Plateau in northern China, is chosen as the study area. The main Weihe River has a total length of 818 km and a drainage area of 1.35×10^4 km^2 (Fig. 1). It originates north of Niaoshu Mountains in Gansu Province and eventually flows into the Yellow River at Tongguan County, Shaanxi Province. The topography of the basin decreases from west to east, with the variation range of elevation being 243–3916 m. There are many tributaries of the Weihe River. The Jinghe River and Beiluo River are the first and second-largest tributaries, respectively. Tributaries with a drainage area of more than 1.00×10^3 km^2 include Bangsha River, Jihe River, Heihe River, Fenghe River, and Bahe River in the south and the Xinhe River, Sandu River, Hulu River, Niutou River, Qianhe River, Qishui River, Shichuan River, Jinghe River, and Beiluo River in the north (Zhou and Yan, 2014). The WRB is located in the transition area between the arid and humid areas of China, with an average annual precipitation of 572 mm. It is characterized by the uneven distribution of more in the south and less in the north. The runoff is also characterized by uneven regional distribution, considerable interannual variation, and uneven annual distribution. The GFG project was first piloted in Gansu, Shaanxi, and Sichuan provinces of China in 1999 and was fully launched nationwide in 2002. Therefore, the large-scale implementation of GFG project in the WRB occurred after 2000.

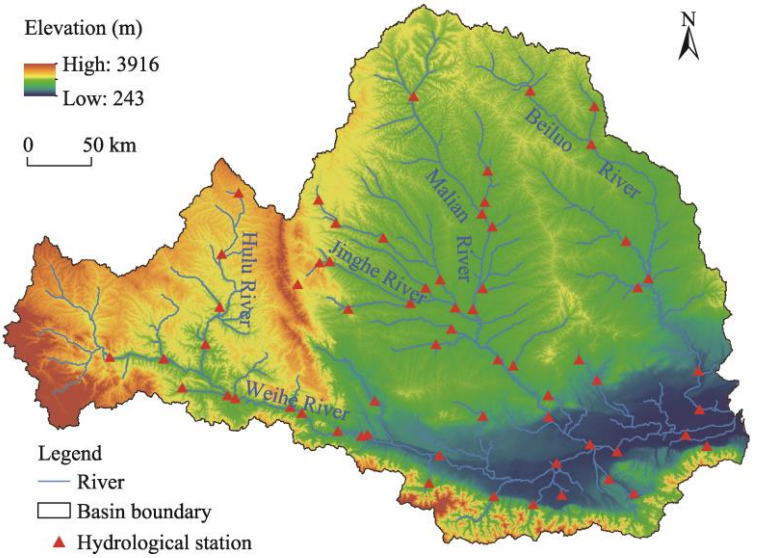

Fig. 1 Topography, river networks, and hydrological stations of the Weihe River Basin (WRB)

2.2 Data sources

To ensure the time consistency and availability of runoff data measured by the selected hydrological station, we chose 2006–2018 as the study period. Daily runoff and precipitation data of hydrological and meteorological stations were acquired from Hydrological Year Book of the

Yellow River Basin (the Ministry of Water Resources of the People's Republic of China, 2006–2018). Other observational daily meteorological data, including daily maximum and minimum air temperatures of 22 national meteorological stations, were derived from the National Meteorological Information Centre, China Meteorological Administration (http://www.cma.gov.cn/). The daily precipitation and temperature data were added or averaged into monthly or annual values for subsequent calculation and analysis.

2.3 Data processing

2.3.1 Runoff characteristic indices

Table 1 lists the 20 indices chosen for this study and their descriptions and calculations. These indices describe the characteristics of runoff from different aspects. Q_1, Q_5, Q_{10}, Q_{20}, Q_{50}, Q_{80}, Q_{90}, Q_{95}, and Q_{99} refer to runoff at 1%, 5%, 10%, 20%, 50%, 80%, 90%, 95%, and 99% exceeding frequencies, respectively. Among them, some are related to high-frequency runoff events (Q_{80}, Q_{90}, Q_{95}, and Q_{99}) and some are related to low-frequency runoff events (Q_1, Q_5, Q_{10}, and Q_{20}). Extreme consecutive daily runoff indices include maximum daily runoff (Max_1), maximum runoff for 7 consecutive days (Max_7), maximum runoff for 30 consecutive days (Max_{30}), minimum daily runoff (Min_1), minimum runoff for 7 consecutive days (Min_7), and minimum runoff for 30 consecutive days (Min_{30}). Additionally, there are also indices showing low runoff variability rate ($R_{Q95:Q50}$) and high runoff variability rate ($R_{Q5:Q50}$). These runoff series can basically reflect the general hydrological characteristics of a watershed (Bassiouni and Oki, 2013).

Table 1 Description and calculation of runoff characteristic indices

Index	Unit	Description and calculation
Q_1, Q_5, Q_{10}, Q_{20}, Q_{50}, Q_{80}, Q_{90}, Q_{95}, and Q_{99}	mm/d	Daily runoff under different exceeding frequencies. The subscript represents the percentage of runoff exceedance probability.
Min_1, Min_7, and Min_{30}	mm	Consecutive minimum daily runoff. The subscript indicates the consecutive days.
Max_1, Max_7, and Max_{30}	mm	Consecutive maximum daily runoff. The subscript indicates the consecutive days.
$R_{Q95:Q50}$ and $R_{Q5:Q50}$	/	Low-runoff variability rate and high-runoff variability rate, respectively. Annual runoff is divided by the median annual runoff, providing an overview of how the flow duration curve changes over time.
RC	/	Ratio of annual runoff to precipitation, reflecting the average water production capacity of the basin during a certain period.
R	mm	Annual runoff.

Note: Q_1, Q_5, Q_{10}, Q_{20}, Q_{50}, Q_{80}, Q_{90}, Q_{95}, and Q_{99} refer to runoff at 1%, 5%, 10%, 20%, 50%, 80%, 90%, 95%, and 99% exceeding frequencies, respectively; Min_1, Min_7, and Min_{30} refer to minimum runoff for 1, 7, and 30 consecutive days, respectively; Max_1, Max_7, and Max_{30} refer to maximum runoff for 1, 7, and 30 consecutive days, respectively; $R_{Q95:Q50}$ and $R_{Q5:Q50}$ refer to low runoff variability rate and high runoff variability rate, respectively; RC refers to runoff coefficient; R refers to annual runoff; "/" denotes dimensionless.

2.3.2 Precipitation- and evaporation- related indicators

To explore which climate factor is most closely related to runoff characteristics, we selected several indicators and their combinations to perform correlation analyses (Table 2). Among climate factors, precipitation is the most active climatic factor in the natural water cycle process, and many precipitation-related factors play an essential role in hydrological processes (Chang et al., 2015). Temperature mainly affects the hydrological process by affecting evaporation. Due to the strong seasonality of precipitation and evaporation, precipitation seasonality (P_{si}) and potential evaporation seasonality ($E_{p\ si}$) were calculated to express their seasonal characteristics. In addition, precipitation and evaporation usually affect runoff through joint action, so the combination of the two was considered. Among the eight selected indicators, three were related to precipitation (annual precipitation, P_{si}, and average rain depth), two were related to evaporation (annual potential evaporation and $E_{p\ si}$), two were related to the combination of precipitation and potential evaporation (aridity index and seasonal correlation between water supply and demand (CORR)), and one to temperature.

Table 2 Climate-related characteristics selected to estimate the runoff characteristics

Predictor	Unit	Calculation
Annual precipitation (P)	mm	$P=\sum_{i=1}^{12} P_i$, where i refers to the month; and P_i is the monthly precipitation (mm).
Precipitation seasonality (P_{si})	/	P_{si} is calculated as follows (Walsh and Lawler, 1981): $P_{si}=P^{-1}\sum\left\|P_i-P/12\right\|$.
Average rain depth (α)	mm/d	Mean precipitation during rainy days.
Annual potential evaporation (E_p)	mm	E_p is calculated by a modified version of the Hargreaves (Droogers and Allen, 2002): $E_p=0.0013\times0.408\times RA\times(T_{av}+17)\times(TD-0.0123P)^{0.76}$, where T_{av} is the average of the mean maximum temperature and minimum temperature for each month (℃); TD represents the difference between the average maximum temperature and minimum temperature per month (℃); and RA represents the extraterrestrial radiation (MJ/(m^2·d)), which were acquired from Food and Agriculture Organization (FAO) of the United Nations.
Potential evaporation seasonality ($E_{p\,si}$)	/	$E_{p\,si}$ is calculated as follows (Walsh and Lawler, 1981): $E_{p\,si}=E_p^{-1}\sum\left\|E_{pm}-E_p/12\right\|$, where E_p and E_{pm} are the annual and monthly potential evaporation (mm), respectively.
Aridity index (ϕ)	/	$\phi=\frac{E_p}{P}$.
Seasonal correlation between water supply and demand (CORR)	/	CORR is the correlation coefficient between monthly precipitation and annual potential evaporation (Petersen et al., 2012).
Average annual temperature (TA)	K	$TA=\sum_{i=1}^{12}(T_i+274.15)/12$, where T_i is the monthly mean air temperature of the i^{th} month (℃).

Note: "/" denotes dimensionless.

2.4 Methods

2.4.1 Flow duration curve (FDC) method

Flow duration curve (FDC) indicates the relationship between the magnitude and the frequency of daily, weekly, monthly, or yearly runoff for a specific watershed without considering the continuity of time, providing a time percentage greater than or equal to a certain flow occurrence in the whole time series (Cigizoglu and Bayazit, 2015). FDC is widely used in hydropower engineering design, water resource supply, irrigation planning, verification of hydrological model results in areas without data, and analysis of regional hydrological characteristics (Vogel and Fennessey, 1994). Based on long time-series daily flows, FDC is one of the most effective methods for analyzing the runoff distribution characteristics and variation in a basin (Gao et al., 2015). FDC was applied in this study to reflect the variation characteristics of watershed runoff comprehensively and graphically during the whole study period.

2.4.2 Correlation analysis

Regression analysis was adopted to evaluate the correlation between runoff values and potential climatic factors listed in Table 2. The choice of linear, exponential, or power functions depends on the determination coefficient (R^2). The fitting equation corresponding to the maximum R^2 is considered the optimal time series distribution.

2.4.3 Trend test

Mann-Kendall (MK) test is a nonparametric method (Mann, 1945; Kendall, 1990). Because this method does not require samples to obey a specific distribution, and the results are not easily disturbed by a few outliers, MK test is widely used in the trend test of hydrological series (Wen et al.,

2019). Gao et al. (2017) introduced the principle and application of this method in detail. In this study, MK test was used to detect the trend of observed runoff series at different gauges in the WRB.

2.4.4 Runoff sensitivity coefficient based on the Budyko framework

Based on the Budyko framework (Budyko, 1974), Fu's function (Fu, 1981) stated that the average annual balance between evaporation and runoff could be presented as follows:

$$F\left(\phi,\omega\right)=\frac{\mathrm{E}}{\mathrm{P}}=1-\frac{\mathrm{R}}{\mathrm{P}}, \tag{1}$$

where E refers to actual evaporation (mm); P represents precipitation (mm); R represents runoff (mm); F is an analytical equation representing the evaporative fraction (E/P) or runoff ratio (R/P); ϕ is aridity index; and ω is a parameter that represents all other factors that affect the average annual distribution of precipitation (such as the type of soil and vegetation and topography).

Rewriting Equation 1, whereby aridity index is replaced by potential evaporation/precipitation (E_p/P) (Berghuijs et al., 2017):

$$\mathrm{R}\left(\mathrm{P},\mathrm{E_P},\omega\right)=\mathrm{P}\left(-\frac{\mathrm{E_P}}{\mathrm{P}}+\left(1+\left(\frac{\mathrm{E_P}}{\mathrm{P}}\right)^{\omega}\right)^{\frac{1}{\omega}}\right), \tag{2}$$

where E_p is potential evaporation (mm).

The elasticity coefficient refers to the ratio of the growth rate of two interrelated indicators in a certain period (Zhang and He, 2016). Then the absolute elasticities of runoff to precipitation, potential evaporation, and other factors were obtained by deriving the partial differential expressions for each factor:

$$\varepsilon_{\mathrm{R,P}}=\frac{\partial \mathrm{R}/\mathrm{R}}{\partial \mathrm{P}/\mathrm{P}}=\frac{\left(\phi^{\omega}+1\right)^{\frac{1}{\omega}-1}}{-\phi+\left(1+\phi^{\omega}\right)^{\frac{1}{\omega}}}, \tag{3}$$

$$\varepsilon_{\mathrm{R,E_p}}=\frac{\partial \mathrm{R}/\mathrm{R}}{\partial \mathrm{E_P}/\mathrm{E_P}}=\frac{\phi^{\omega}\left(\phi^{\omega}+1\right)^{\frac{1}{\omega}-1}-\phi}{-\phi+\left(1+\phi^{\omega}\right)^{\frac{1}{\omega}}}, \tag{4}$$

$$\varepsilon_{\mathrm{R},\omega}=\frac{\partial \mathrm{R}/\mathrm{R}}{\partial \omega/\omega}=\frac{\left(\phi^{\omega}+1\right)^{\frac{1}{\omega}}\times\left(\frac{\phi^{\omega}\ln\left(\phi\right)}{\phi^{\omega}+1}-\frac{\ln\left(\phi^{\omega}+1\right)}{\omega}\right)}{-\phi+\left(1+\phi^{\omega}\right)^{\frac{1}{\omega}}}, \tag{5}$$

where ω represents other factors; $\varepsilon_{\mathrm{R,P}}$, $\varepsilon_{\mathrm{R,Ep}}$, and $\varepsilon_{\mathrm{R},\omega}$ are the absolute sensitivities of runoff to precipitation, potential evaporation, and other factors, respectively.

To assess the relative importance of each influencing factor, the calculation of the relative sensitivity of runoff to these three factors is as follows:

$$\theta_x=\frac{\left|\varepsilon_{R,\mathrm{x}}\right|}{\left|\varepsilon_{R,\omega}\right|+\left|\varepsilon_{R,E_p}\right|+\left|\varepsilon_{R,P}\right|}, \tag{6}$$

where θ_x is the relative sensitivity of runoff to precipitation, potential evaporation, and other factors. θ_x can vary from close to zero (i.e., almost unaffected by that specific factor) to close to one (i.e., almost completely affected by that specific factor).

3 Results

3.1 Temporal and spatial characteristics of runoff

3.1.1 Exceedance frequency for daily runoff

Figure 2 shows the flow duration curves (FDCs) of daily runoff for 62 hydrological stations in the

WRB during 2006–2018. The FDCs of the selected hydrological stations fell in three narrow bands with mean annual runoff values of 3.43–13.33 mm, 20.92–109.30 mm, and 229.03–507.25 mm, represented by red, green, and blue lines, respectively. The results depicted significant variabilities in runoff in different areas of the WRB. Among them, the green curves accounted for the highest proportion, showing that the runoff variability at most stations was in the middle range. Between Q_{20} and Q_{80}, the slopes of FDCs were relatively gradual. The value of Q_{50} varied from 0.00 to 0.79 mm. For high-frequency runoff events (Q_{90}, Q_{95}, and Q_{99}) and rare-frequency runoff events (Q_1, Q_5, and Q_{10}), the FDCs of each station decreased as the percentage of exceedance increased. It can be seen that in the upstream area of each tributary, including the main stem of the Weihe River, Hulu River, and Malian River in the northern Jinghe River Basin, the runoff was low. The high-runoff areas were mainly located on the south bank of the WRB, including the Bahe River, Laohe River, Fenghe River, and Shitou River.

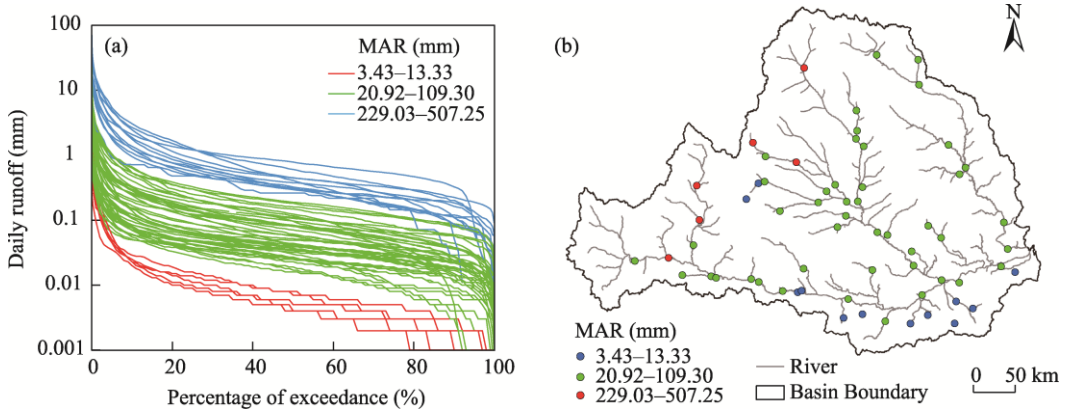

Fig. 2 (a), flow duration curves (FDCs) of daily runoff in the WRB with three distinct ranges of mean annual runoff (MAR); (b), spatial distribution of hydrological stations with different ranges of MAR. Red, green, and blue sites are 6, 45, and 11 of the 62 stations, respectively, where MAR varied from 3.43 to 13.33 mm, from 20.92 to 109.30 mm, and from 229.03 to 507.25 mm, respectively.

3.1.2 Trend of daily runoff at different exceedance frequencies

We divided the WRB into 62 subintervals based on the selected hydrological stations. The area controlled by a single hydrological station was divided into one interval; and the area between adjacent hydrological stations upstream and downstream of the river was divided into an interval. During the study period, the variation trends of Q_{95}, Q_{50}, and Q_5 in different intervals are shown in Figure 3. For high-frequency runoff events (Q_{95}), 17 subintervals showed significant upward trends, which were located at the source of the WRB, the middle and lower reaches of the Jinghe River Basin, and the middle reaches of Beiluo River Basin; 2 subintervals showed a downward trend, and other subintervals showed no significant trend. For intermediate-frequency runoff events (Q_{50}), nine subintervals showed a significant upward trend, most of them were located in the Jinghe River Basin; two subintervals showed a downward trend, and others showed no trends.

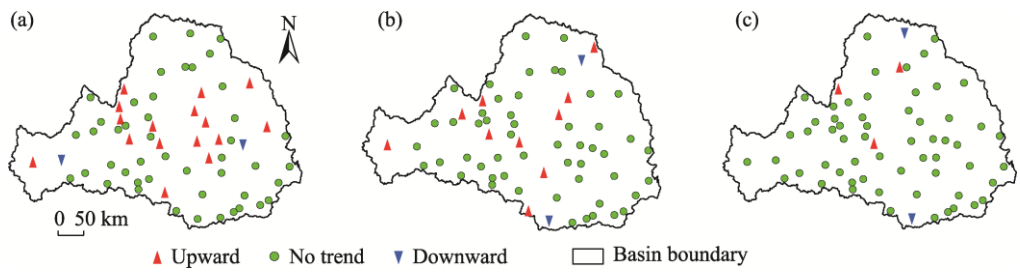

Fig. 3 Spatial distributions of runoff trends under high-frequency runoff events (Q_{95}; a), intermediate-frequency runoff events (Q_{50}; b), and rare-frequency runoff events (Q_5; c)

For rare-frequency runoff events (Q_5), three subintervals showed significant upward trends, and two showed a downward trend. In general, the runoff on the south bank of the Weihe River was more stable than that on the north bank, and high-frequency runoff events had more variability than intermediate- and rare- frequency runoff events.

3.1.3 Seasonal distribution of annual precipitation and runoff

Taking the observed runoff at Linjiacun, Xianyang, and Huaxian stations located in the upper, middle, and lower reaches of the main stream of the Weihe River, respectively, Zhangjiashan station in the Jinghe River Basin and Zhuangtou station in the Beiluo River Basin as examples, and taking the sum of observed runoff of Huaxian and Zhuangtou stations as the total runoff of the whole WRB, the monthly distribution of precipitation and runoff was analyzed (Table 3). For the selected hydrological stations, the monthly precipitation and runoff were distributed unevenly and mainly concentrated in the flood season (June–September) (Table 3). Precipitation in the flood season accounted for more than 60.00% of the average annual precipitation for the year. Runoff from June to September accounted for approximately 50.00% of the total flow volume. The results revealed the nonuniformity of the annual distribution of the WRB.

Table 3 Distribution of monthly precipitation and runoff in the Weihe River basin (WRB)

Station	Hydrological element	Jan (mm)	Feb (mm)	Mar (mm)	Apr (mm)	May (mm)	Jun (mm)	Jul (mm)	Aug (mm)	Sep (mm)	Oct (mm)	Nov (mm)	Dec (mm)	Proportion in flood season (%)
Linjiacun	Precipitation	6.75	12.36	28.45	42.01	67.83	79.81	125.67	117.11	129.45	51.22	19.95	3.34	66.09
	Runoff	1.14	0.82	1.18	1.68	2.26	2.11	5.86	4.14	4.47	3.48	1.70	1.34	54.94
Xianyang	Precipitation	6.38	9.91	23.41	36.78	60.26	54.16	103.21	100.87	105.06	47.98	20.56	3.67	63.49
	Runoff	2.03	1.77	2.07	3.21	3.97	4.05	8.22	7.25	11.29	7.64	4.26	2.69	52.71
Huaxian	Precipitation	4.36	8.85	17.37	36.79	59.82	50.17	90.58	79.21	98.98	43.32	26.11	4.48	61.33
	Runoff	1.86	1.53	1.84	2.95	3.54	2.78	6.36	6.04	8.95	6.01	3.62	2.26	50.54
Zhangjiashan	Precipitation	6.48	9.48	23.07	34.05	47.83	56.15	88.88	75.76	95.82	38.58	18.12	3.34	63.63
	Runoff	0.97	1.11	1.60	1.28	1.18	1.21	4.05	3.83	3.33	2.29	1.68	1.23	52.27
Zhuangtou	Precipitation	4.20	8.80	13.24	29.63	50.93	54.05	87.05	77.34	82.67	42.42	20.36	2.19	63.68
	Runoff	0.82	0.99	1.68	1.39	1.16	1.06	3.19	2.99	3.12	2.18	1.51	1.16	48.75
Total	Precipitation	5.64	9.88	21.11	35.85	57.34	58.87	99.08	90.06	102.40	44.70	21.02	3.40	63.79
	Runoff	0.99	0.94	1.29	1.53	1.69	1.52	3.85	3.50	4.41	3.03	1.87	1.26	51.31

3.1.4 Trend analysis of annual runoff in different subintervals

The annual runoff trend analysis in the WRB is shown in Figure 4. The regions with significantly increasing inflow were distributed in the middle and upper reaches of the Beiluo River Basin, the upper reaches of the Jing River, and the south bank of the Weihe River. The regions with significantly decreasing inflow were distributed in the lower reaches of the Beiluo River and the upper reaches of the Weihe River. In most regions, the runoff showed no significant trend in the study period.

3.2 Climate-related factors on runoff variability

Taking the total runoff of the WRB, the effects of climate-related factors on runoff variability were analyzed. Table 4 lists the R^2 values between the runoff characteristics and precipitation- and evaporation- related control factors. According to the average value of R^2 sorted from high to low, the three principal factors affecting runoff were precipitation, aridity index, and runoff depth in rainy days, while the three least important influencing factors were precipitation seasonality, potential evaporation seasonality, and potential evaporation. In general, the factors related to precipitation have the greatest impact on runoff, while the factors related to evaporation are less informative. Each influencing factor performed differently toward every runoff characteristic index. The most important influencing factors for rare-frequency daily runoff events (Q_1, Q_5, Q_{10},

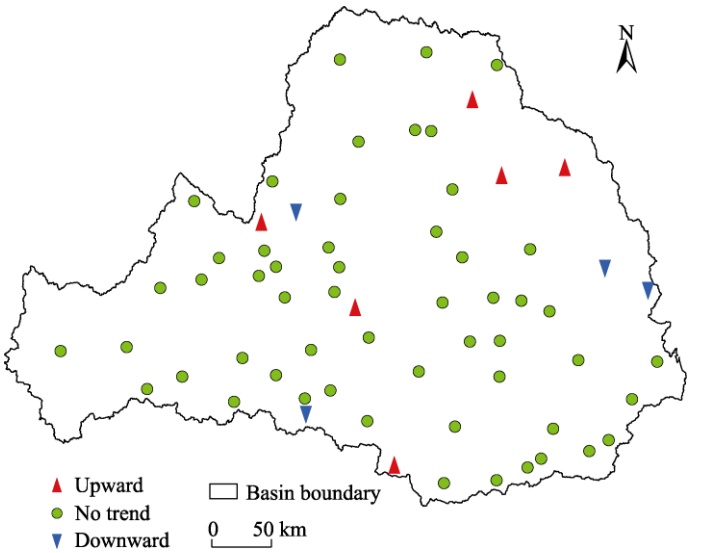

Fig. 4 Spatial distributions of annual runoff trends in different subintervals

Table 4 R^2 values between runoff characteristics and climate-related factors

Index	P	P_{si}	α	E_p	$E_{p\,si}$	ϕ	CORR	TA
Q_1	0.72^{+}_{lin}	0.22^{+}_{pow}	0.64^{+}_{pow}	0.20^{-}_{pow}	0.06^{-}_{pow}	0.69^{-}_{pow}	0.46^{+}_{exp}	0.29^{-}_{pow}
Q_5	0.72^{+}_{pow}	0.16^{+}_{pow}	0.70^{+}_{lin}	0.17^{-}_{pow}	0.14^{-}_{log}	0.64^{-}_{pow}	0.34^{+}_{log}	0.17^{-}_{exp}
Q_{10}	0.78^{+}_{pow}	0.14^{+}_{pow}	0.63^{+}_{pow}	0.16^{-}_{exp}	/	0.69^{-}_{pow}	0.34^{+}_{log}	0.22^{-}_{exp}
Q_{20}	0.68^{+}_{exp}	0.06^{+}_{pow}	0.32^{+}_{pow}	0.25^{-}_{exp}	0.05^{+}_{lin}	0.49^{-}_{pow}	0.20^{+}_{log}	0.42^{-}_{exp}
Q_{50}	0.06^{+}_{pow}	0.22^{+}_{lin}	/	0.30^{-}_{exp}	/	0.12^{-}_{exp}	0.06^{+}_{lin}	0.43^{-}_{exp}
Q_{80}	/	0.18^{+}_{lin}	0.08^{-}_{lin}	0.06^{-}_{lin}	/	/	0.05^{+}_{lin}	0.21^{-}_{log}
Q_{90}	/	0.15^{+}_{lin}	/	/	/	/	0.15^{+}_{lin}	0.12^{-}_{lin}
Q_{95}	/	0.07^{+}_{lin}	/	/	0.06^{-}_{lin}	/	0.15^{+}_{lin}	0.09^{+}_{lin}
Q_{99}	/	/	/	0.07^{+}_{exp}	0.07^{-}_{lin}	/	0.19^{+}_{lin}	/
Max_1	0.58^{+}_{exp}	0.35^{+}_{pow}	0.48^{+}_{exp}	0.23^{-}_{pow}	/	0.59^{-}_{pow}	0.50^{+}_{lin}	0.37^{-}_{exp}
Max_7	0.81^{+}_{exp}	0.18^{+}_{pow}	0.66^{+}_{pow}	0.15^{-}_{pow}	/	0.75^{-}_{pow}	0.38^{+}_{lin}	0.23^{-}_{exp}
Max_{30}	0.75^{+}_{pow}	0.18^{+}_{pow}	0.62^{+}_{pow}	0.17^{-}_{pow}	/	0.72^{-}_{pow}	0.42^{+}_{lin}	0.26^{-}_{exp}
Min_1	/	/	/	/	0.15^{-}_{lin}	/	0.22^{+}_{lin}	/
Min_7	/	/	0.04^{+}_{pow}	0.08^{+}_{exp}	0.07^{-}_{lin}	/	0.11^{+}_{lin}	/
Min_{30}	0.07^{-}_{lin}	/	0.13^{-}_{lin}	/	/	/	0.05^{+}_{lin}	0.05^{-}_{lin}
$R_{Q95:Q50}$	0.08^{+}_{pow}	/	0.12^{+}_{pow}	0.06^{-}_{pow}	/	0.19^{+}_{exp}	/	0.12^{+}_{pow}
$R_{Q5:Q50}$	0.71^{+}_{pow}	0.09^{+}_{lin}	0.75^{+}_{pow}	0.07^{-}_{pow}	0.12^{-}_{log}	0.57^{-}_{pow}	0.28^{+}_{pow}	0.05^{-}_{exp}
RC	0.40^{+}_{lin}	0.17^{+}_{exp}	0.22^{+}_{pow}	0.25^{-}_{pow}	/	0.27^{-}_{pow}	0.26^{+}_{lin}	0.56^{-}_{exp}
MAR	0.69^{+}_{pow}	0.13^{+}_{exp}	0.45^{+}_{pow}	0.23^{-}_{pow}	/	0.62^{-}_{pow}	0.35^{+}_{lin}	0.36^{-}_{exp}

Note: P, annual precipitation; P_{si}, precipitation seasonality; α, average rain depth; E_p, annual potential evaporation; $E_{p\,si}$, potential evaporation seasonality; ϕ, aridity index; CORR, seasonal correlation between water supply and demand; TA, average annual temperature. Different fitting functions were considered here. "Lin", "exp", "log", and "pow" represent linear, exponential, logarithm, and power functions, respectively. Only the values of R^2 with the strongest correlation are displayed. "/" denotes R^2<0.05; "+" and "–" indicate positive and negative relationships between runoff characteristics and climate-related factors, respectively.

and Q_{20}), consecutive maximum daily runoff events (Max_1, Max_7, and Max_{30}), and high streamflow variability ($R_{Q5:Q50}$) were precipitation, aridity index, and runoff depth in rainy days. Influencing factors identified as important for runoff coefficient were precipitation and annual average temperature. However, no significant influencing factors were detected for intermediate-

and high-frequency runoff events (Q_{50}, Q_{80}, Q_{90}, Q_{95}, and Q_{99}), minimum consecutive daily runoff (Min_1, Min_7, and Min_{30}), and low streamflow variability rates ($R_{Q95:Q50}$).

3.3 Sensitivity analysis of runoff to its potential influencing factors

3.3.1 Spatial hydroclimatic characteristics

The spatial distribution characteristics of the average runoff ratio, aridity index, and other factors during 2006–2018 are shown in Figure 5. Different values were graded by natural discontinuities in ArcGIS 10.2. The runoff ratio in most areas of the WRB was 0.05–1.00, accounting for approximately half of the total hydrological stations. The value of aridity index was concentrated in 1.30–1.50, matching the climate conditions in the arid and semi-arid areas of the WRB. The spatial distribution characteristics of aridity index and runoff ratio were opposite. The runoff ratio was usually small in places with high aridity index, such as the northern WRB. Other factors showed the characteristics of high in the north and low in the south of the Weihe River.

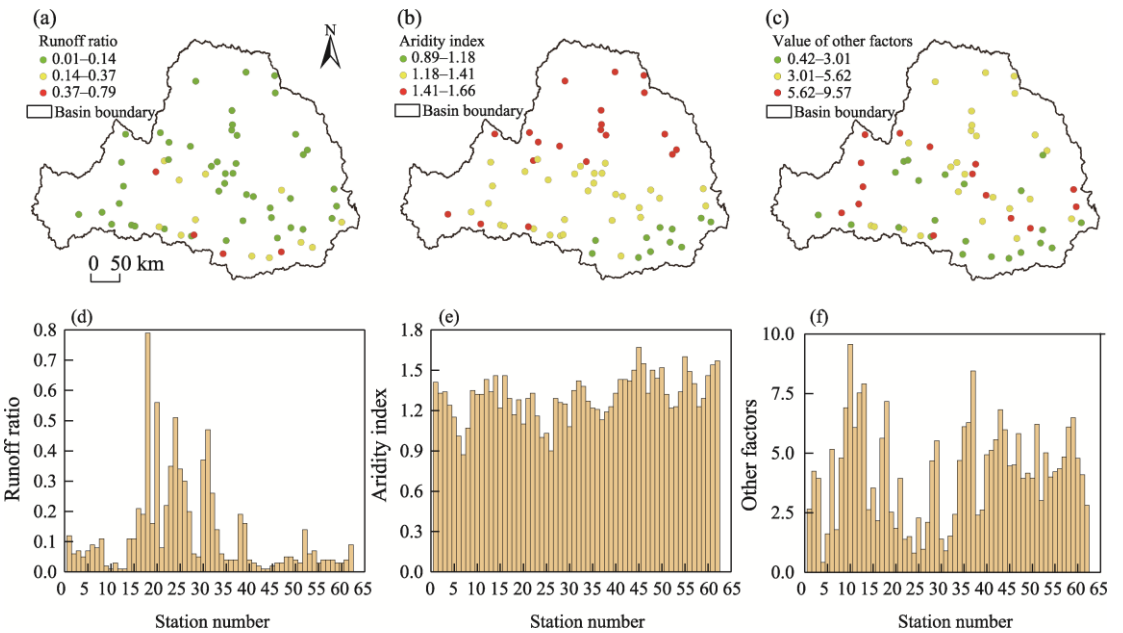

Fig. 5 Distribution of spatial hydrological and climatic characteristics in the study area based on the Budyko framework. (a–c), spatial pattern of the runoff ratio, aridity index, and other factors, respectively; (d–f), values of the runoff ratio, aridity index, and other factors at different hydrological stations, respectively.

3.3.2 Spatial pattern of absolute runoff elasticities

Based on the obtained aridity index and other factors (Fig. 5), we depicted the spatial distribution of the sensitivities of runoff to precipitation, potential evaporation, and other factors in Figure 6. The stations with a sensitivity of runoff to precipitation ($\varepsilon_{R,P}$) greater than 1.00 accounted for about 93.55% of the observed stations, suggesting that the change in runoff caused by precipitation was always equal to or larger than the change in precipitation itself. The average value of $\varepsilon_{R,P}$ was 3.85, indicating that an increase of 10.00% in precipitation would lead to a 38.50% increase in runoff. Generally, relatively humid regions (aridity index<1.20) have lower $\varepsilon_{R,P}$ values (e.g., the southern region of the basin). The WRB is a typical arid and semi-arid transitional zone in China, and the runoff of this area has a far higher sensitivity to precipitation changes. In addition, $\varepsilon_{R,P}$ always exceeded the absolute sensitivity of runoff to potential evaporation ($\varepsilon_{R,Ep}$), suggesting that the percentage change in runoff caused by precipitation was greater than that caused by potential evaporation. Compared with precipitation, potential evaporation has an opposite effect on runoff. The average $\varepsilon_{R,Ep}$ was –2.85, indicating that an increase of 10.00% in precipitation would lead to a 28.50% decrease in runoff. Runoff in

relatively humid areas showed higher sensitivity to potential evaporation than in arid regions. The elasticity of runoff to other factors ($\varepsilon_{R,\omega}$) was similar to that to $\varepsilon_{R,Ep}$, with a mean value of –2.16. Li et al. (2021) proved that other factors was significantly correlated with climatic and artificial factors. $\varepsilon_{R,\omega}$ was generally lower in dryland regions (e.g., the north of the Beiluo River and Jinghe River Basin) and higher in relatively humid areas (e.g., the south of the WRB). The sensitivity analysis showed that precipitation could promote runoff, while potential evaporation and other factors inhibited runoff.

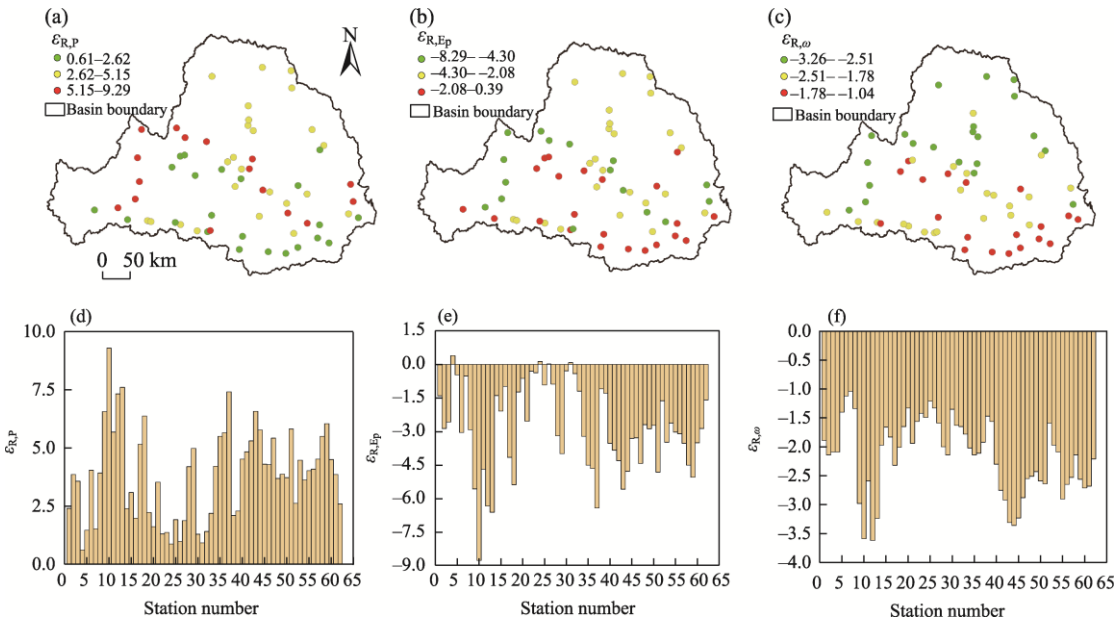

Fig. 6 Absolute sensitivities of runoff to precipitation ($\varepsilon_{R,P}$; a), annual potential evaporation ($\varepsilon_{R,Ep}$; b), and other factors ($\varepsilon_{R,\omega}$; c) in the WRB. (d–f), values of $\varepsilon_{R,P}$, $\varepsilon_{R,Ep}$, and $\varepsilon_{R,\omega}$ at different hydrological stations, respectively.

3.3.3 Relative sensitivity of runoff to the precipitation, potential evaporation, and other factors

The relative sensitivities of runoff to precipitation (θ_P), potential evaporation (θ_{Ep}), and other factors (θ_ω) are showed in Figure 7. For 87.10% of the selected hydrological stations, precipitation was always the most critical contributor to runoff changes ($\theta_P > \theta_{Ep}$ and θ_ω), while the other factors were the dominant factor for the remaining 12.90% of the selected hydrological stations ($\theta_\omega > \theta_P$ and θ_{Ep}). There was no land area that potential evaporation accounted for the most part.

4 Discussion

4.1 Impact of climate-related factors on runoff variability

Runoff is highly variable in different intervals of the study area, which may be related to the local differences in soil texture, landform, runoff mechanism, watershed size, and river network density (Rossi et al., 2016). For a specific watershed, the landform and soil properties are relatively stable in a short period, and the vegetation cover will not change significantly. Therefore, meteorological elements have become essential factors affecting hydrological processes (Liu et al., 2016). Among them, precipitation plays a vital role in the hydrological cycle process. The results of the correlation analysis showed that precipitation-related factors greatly impacted runoff change (Table 4). To show the relationship between daily runoff and daily precipitation more clearly, we constructed the FDCs for daily precipitation at 62 meteorological stations (Fig. 8). Because there are many days with no rainfall in a year, the diagram was drawn only for rainy days. There was substantial overlap among precipitation events when mean annual runoff varied across 3.00 orders of magnitude (Fig. 2), suggesting that precipitation among stations was relatively stable.

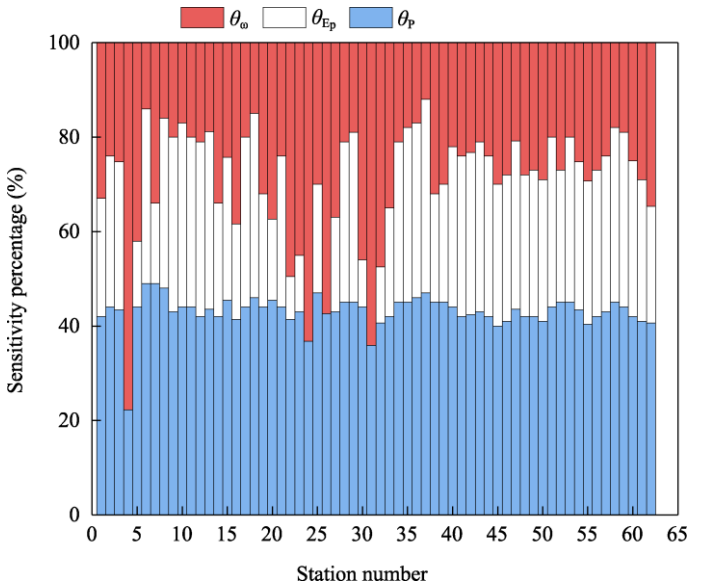

Fig. 7 Relative sensitivities of runoff to precipitation (θ_P), potential evaporation (θ_{Ep}), and other factors (θ_ω) at different hydrological stations

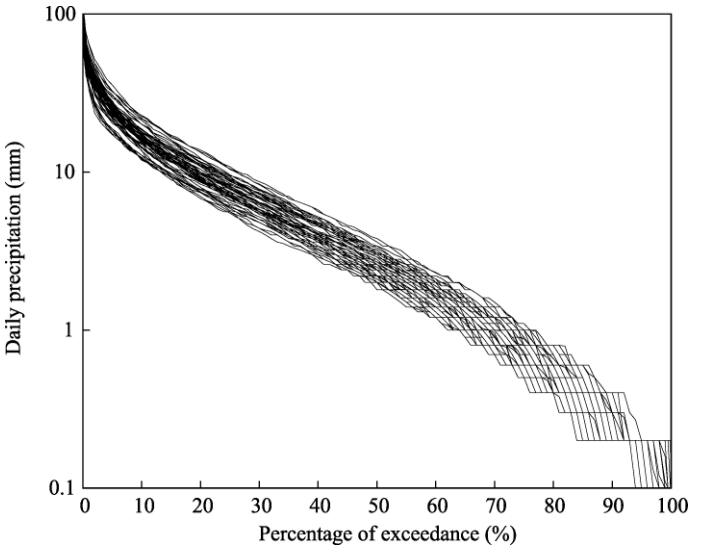

Fig. 8 FDCs for daily precipitation of 62 meteorological stations in the WRB

The shape of the curves showed that precipitation has a firm consistency with the rare-frequency runoff events, indicating that the influence of extreme precipitation events on rare-frequency runoff was more potent than that on intermediate- and high- frequency runoff events. High-frequency runoff events, such as Q_{95} and Q_{99}, are usually regarded as the base flow (Beck et al., 2015), which is relatively stable and not easily affected.

Daily precipitation can also be described by the proportion of wet to dry days representing rain frequency (f) and average precipitation depth on rainy days (α) (Rossi et al., 2016). Based on the resulting values, we transformed mean annual precipitation, α, and f into grid maps by the Kriging method in ArcGIS10.2 (Hevesi et al., 1992) (Fig. 9). It showed that the areas with high mean annual precipitation were sometimes related to large α (e.g., high α in the middle Beiluo River), high f (e.g., high f in the Hulu River), or both (e.g., south bank of the Weihe River), which illustrated that mean annual precipitation is affected by extreme weather conditions. The precipitation in the south and east of the WRB was more abundant than that in the north and west.

Combined with the spatial distribution of runoff characteristics, this may be the reason why the runoff was greater in the south than in the north, more in the east, and less in the west (Fig. 5). However, Rossi et al. (2016) found that rainfall variability played a secondary role in runoff variability. The most important driving force for daily runoff variation may be the nonlinear transformation from precipitation to runoff, rather than the daily rainfall statistics. Additionally, precipitation also influences runoff generation by affecting the soil water content, vegetative cover, evapotranspiration, etc. (Rodriguez-Iturbe, 2000).

Figure 9 f shows the spatial distribution of other climate-related factors. In the higher altitude areas, the CORR was high, while potential evaporation and annual temperature was low. Potential evaporation was large in the northern WRB, but annual temperature was not the highest. From the results of the correlation analysis (Table 4), CORR, potential evaporation, and annual temperature have poor correlations with runoff. Potential evaporation and annual temperature have adverse effects on runoff, while CORR has positive effects.

The temporal variations in precipitation and potential evaporation are usually considered the leading causes of runoff and evaporation changes over time (Greve et al., 2014). Evaporation is a term balancing input precipitation, which may strongly affect the conversion of precipitation into runoff at a daily scale to adjust runoff variability (Samain and Pauwels, 2013). Aridity index, calculated by precipitation and potential evaporation, determined the spatial distribution of precipitation to runoff and evaporation (Budyko, 1974; Greve et al., 2014). In general, various climate factors are interrelated and interact with each other, leading to the variation in runoff. With the advancement of global warming, the atmospheric water content will increase, which will make further efforts on the Earth's water cycle (Huntington et al., 2016). Therefore, the spatiotemporal distribution of runoff would be consequently affected (Zhang and Dong, 2013).

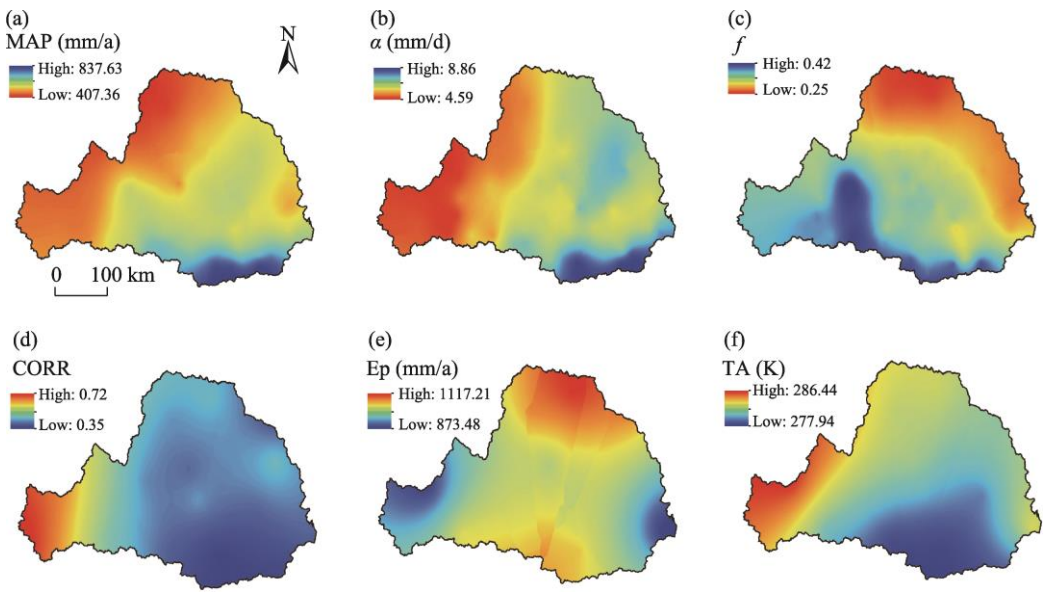

Fig. 9 Spatial distribution of mean annual precipitation (MAP; a), mean precipitation in rainy days (α; b), the ratio of wet to dry days (f; c), the seasonal correlation between water supply and demand (CORR; d), mean annual potential evaporation (Ep; e), and average annual temperature (TA; f) in the WRB

4.2 Explanations for temporal and spatial variabilities of runoff

In the WRB, the difference in runoff on a time scale was not significant, but it showed distinct regional characteristics in space. Runoff from the southern and western rivers was more abundant and stable than that from the northern and eastern rivers (Figs. 2 and 3). The reasons for this may be explained as follows.

First, there is a difference between geological and geomorphic conditions. The north bank of

the Weihe River is densely distributed with river networks, most of which mainly flow through the hilly and gully areas of the Loess Plateau and Guanzhong Plain. The role of loose loess soil and sparse vegetation in the distribution and regulation of precipitation on the Loess Plateau makes the annual runoff in this region smaller, but the interannual variation is larger (Bai et al., 2020). The alluvial plain of the Weihe River is very flat, with a high degree of water conservancy, belonging to the low water yield area (Wu et al., 2022). The tributaries on the south bank originate from the northern foot of the Qinling Mountains, with short sources, rapid flow, steep rise and fall of the river, and good conditions for runoff production and confluence, such as the Qingjiang River, Heihe River, Laoyu River, Dayu River, and Luofu River. Coupled with small rainfall loss and abundant recharge, the south bank of the Weihe River was considered a high water-yield area in the WRB (Gao and Feng, 2019; Wu et al., 2022). The southern WRB covers an area of 1.48×10^6 km^2, with a total of 3.84×10^9 m^3 of self-produced water resources, accounting for approximately half of the total water resources in the Guanzhong area, which provides water for life, production, and ecology (Gao and Feng, 2019).

Second, the different intensities of human activities. The intensity of human activities on the south bank of the Weihe River is weak, and the degree of development and utilization of water resources is relatively lower. The nonagricultural population accounts for only approximately 10% of the total population in the region, and the per capita regional Gross Domestic Product (GDP), local fiscal revenue, and urban and rural residents' income are lower than the average level of Shaanxi Province of China (Gao and Feng, 2019). For the north bank, the population of the Guanzhong Plain is about 2.0×10^7, the local population density is as high as 800/km^2, and the population urbanization rate is about 60.00% (Jia and Yang, 2017). Sustained population growth, urban scale expansion, and industrial structure upgrading all have a large water demand (Gao et al., 2013; Zhan et al., 2014; Wang et al., 2019). Additionally, the Guanzhong Plain has a long history of irrigation, which is the principal form of water consumption. Irrigation water on the Guanzhong Plain accounted for 48.65% of the total water consumption in 2019 (Shaanxi Province Department of Water Resources, 2019).

Since the 1970s, a large-scale GFG project has been implemented in the WRB, which has significantly changed the land use/land cover conditions and improved the regional ecological environment (Li et al., 2017; Jiang et al., 2021). By increasing the soil surface roughness, slowing the runoff speed, increasing infiltration, and intensifying evaporation, runoff was restrained (Yang et al., 2021). Compared with the south bank, the GFG project has been implemented more widely in the loess area on the north bank and has achieved more significant results (Zhang et al., 2018). Some researchers have proposed that excessive vegetation restoration may be a poor choice in arid and semi-arid areas because local precipitation conditions are not considered, which exacerbates the shortage of water resources to a certain extent (Jiang et al., 2019). In this study, the annual runoff entered a relatively stable low-flow period, with no significant trend from 2006 to 2018. For seasonal distribution, runoff usually accounts for a large proportion in the flood season with abundant rainfall, which is consistent with most studies (Gao et al., 2013; Xie et al., 2022). The runoff coefficient of the basin was relatively low during the study period, varying from 0.05 to 0.11, which is smaller than the existing study (Feng et al., 2016), suggesting that the ability of precipitation to transform into the runoff is weakened. Therefore, large-scale vegetation restoration programs need effective and sustainable management.

5 Conclusions

Based on the measured daily runoff and meteorological data of 62 gauges in the WRB from 2006 to 2018, we analyzed the runoff characteristics and the correlations between the runoff characteristic indicators and climate-related factors in this study. The modified Budyko framework was applied to evaluate the sensitivities of runoff to precipitation, potential evaporation, and other factors. The main findings are as follows.

(1) Under different exceedance frequencies, the runoff of different hydrological stations in the

WRB varied greatly. The FDCs of the selected 62 hydrological stations fall in three narrow bands, with the mean annual runoff spanning approximately 1.50 orders of magnitude. The runoff on the south bank of the Weihe River was more abundant and stable than that on the north bank, which is the primary water source of the WRB.

(2) Precipitation-related factors have more influence on runoff characteristics than evaporation-related factors. In this study, rare-frequency runoff events (Q_1, Q_5, Q_{10}, and Q_{20}), consecutive maximum daily runoff (Max_1, Max_7, and Max_{30}), and the ratio of high-runoff variability ($R_{Q5:Q50}$) were strongly related to precipitation, aridity index, and average precipitation depth on rainy days, while high-frequency runoff events (Q_{50}, Q_{80}, Q_{90}, Q_{95}, and Q_{99}), consecutive minimum daily runoff (Min_1, Min_7, and Min_{30}), and the ratio of low-runoff variability ($R_{Q95:Q50}$) had little correlation with the influencing factors.

(3) Compared with potential evaporation and other factors, runoff was more sensitive to precipitation. In this study, the runoff of 87.10% of the hydrological stations was the most sensitive to precipitation, while the remaining 12.90% was dominated by other factors. Aridity index is an important factor affecting runoff characteristics. In places with lower aridity index, such as the south bank of the WRB, runoff was more sensitive to potential evaporation and other factors than to precipitation. Potential evaporation and other factors had adverse effects, while precipitation had positive effects on runoff. In general, runoff change is comprehensively affected by various factors.

Acknowledgements

This work was funded by the National Natural Science Foundation of China (U2243211).

References

Bai Y P, Zhao G J, Zhang L M, et al. 2020. Spatiotemporal variation of sediment load in the Weihe River Basin in recent 55 years and the driving factors. Journal of Soil and Water Conservation, 34(4): 91–97. (in Chinese)

Bassiouni M, Oki D S. 2013. Trends and shifts in streamflow in Hawai'i, 1913–2008. Hydrological Processes, 27(10): 1484–1500.

Beck H E, De Roo A, Van Dijk A. 2015. Global maps of streamflow characteristics based on observations from several thousand catchments. Journal of Hydrometeorology, 16(4): 1478–1501.

Berghuijs W R, Larsen J R, Emmerik T H, et al. 2017. A global assessment of runoff sensitivity to changes in precipitation, potential evaporation, and other factors. Water Resources Research, 53(10): 8475–8486.

Budyko M I. 1974. Climate and Life. San Diego: Academic Press.

Chang J, Wang Y, Istanbulluoglu E, et al. 2015. Impact of climate change and human activities on runoff in the Weihe River Basin, China. Quaternary International, 380: 169–179.

Cigizoglu H K, Bayazit M. 2015. A generalized seasonal model for flow duration curve. Hydrological Processes, 14(6): 1053–1067.

Droogers P, Allen R G. 2002. Estimating reference evapotranspiration under inaccurate data conditions. Irrigation and Drainage Systems, 16(1): 33–45.

Feng X M, Fu B J, Piao S L, et al. 2016. Revegetation in China's Loess Plateau is approaching sustainable water resource limits. Nature Climate Change, 6: 1019–1022.

Fu B P. 1981. On the calculation of the evaporation from land surface. Scientia Atmospherica Sinica, 5: 23–31. (in Chinese)

Gao P, Geissen V, Ritsema C J, et al. 2013. Impact of climate change and anthropogenic activities on stream flow and sediment discharge in the Wei River basin, China. Hydrology and Earth System Sciences, 17(3): 961–972.

Gao P, Jiang G T, Wei Y P, et al. 2015. Streamflow regimes of the Yanhe River under climate and land use change, Loess Plateau, China. Hydrological Processes, 29(10): 2402–2413.

Gao P, Li P F, Zhao B L, et al. 2017. Use of double mass curves in hydrologic benefit evaluations. Hydrological Processes, 31(26): 4639–4646.

Gao X Y, Feng C L. 2019. An assumption for the plan on constructing water ecological corridor in the south bank of Weihe River (Shaanxi section). Water Resources Development and Management, 3: 6–11. (in Chinese)

Greve P, Orlowsky B, Mueller B, et al. 2014. Global assessment of trends in wetting and drying over land. Nature Geoscience,

7(10): 716–721.

Hevesi J A, Istok J D, Flint A L. 1992. Precipitation estimation in mountainous terrain using multivariate geostatistics. Part I: Structural Analysis. Journal of Applied Meteorology, 31(7): 661–676.

Huang Z W, Yang H B, Yang D W. 2016. Dominant climatic factors driving annual runoff changes at the catchment scale across China. Hydrology and Earth System Sciences, 20(7): 2573–2587.

Huntington J, Mcgwire K, Morton C, et al. 2016. Assessing the role of climate and resource management on groundwater dependent ecosystem changes in arid environments with the Landsat archive. Remote Sensing of Environment, 185: 186–197.

Jia Y Y, Yang J P. 2017. The prediction on housing demand caused by population change in Guanzhong urban agglomeration. Land Development and Engineering Research, 2(8): 27–32.

Jiang C, Zhang H Y, Wang X C, et al. 2019. Challenging the land degradation in China's Loess Plateau: Benefits, limitations, sustainability, and adaptive strategies of soil and water conservation. Ecological Engineering, 127: 135–150.

Jiang C, Yang Z Y, Li M T, et al. 2021. Exploring soil erosion trajectories and their divergent responses to driving factors: a model-based contrasting study in highly eroded mountain areas. Environmental Science and Pollution Research, 28(12): 14720–14738.

Kendall M G. 1990. Rank correlation methods. British Journal of Psychology, 25(1): 86–91.

Li F P, Zhang G X, Dong L Q. 2013. Studies for impact of climate change on hydrology and water resources. Scientia Geographica Sinica, 33(4): 457–464. (in Chinese)

Li H J, Shi C X, Sun P C, et al. 2021. Attribution of runoff changes in the main tributaries of the middle Yellow River, China, based on the Budyko model with a time-varying parameter. CATENA, 206: 105557, doi: 10.1016/j.catena.2021.105557.

Li J J, Peng S Z, Li Z. 2017. Detecting and attributing vegetation changes on China's Loess Plateau. Agricultural and Forest Meteorology, 247: 260–270.

Li L, Ni J R, Chang F, et al. 2020. Global trends in water and sediment fluxes of the world's large rivers. Science Bulletin, 65(1): 62–69.

Li S Y, Yang G Y, Wang H. 2019. The runoff evolution and the differences analysis of the causes of runoff change in different regions: A case of the Weihe River Basin, Northern China. Sustainability, 11(19): 5295, doi: 10.3390/su11195295.

Li Y Y, Chang J X, Wang Y M, et al. 2016. Spatiotemporal impacts of climate, land cover change and direct human activities on runoff variations in the Wei River Basin, China. Water, 8(6): 220, doi: 10.3390/w8060220.

Li Z W, Xu X L, Yu B F, et al. 2016. Quantifying the impacts of climate and human activities on water and sediment discharge in a karst region of Southwest China. Journal of Hydrology, 542(11): 836–849.

Liu J K, Zhang Z M, Yan G X, et al. 2016. Multi-scale analysis on precipitation-runoff relationship in Chaobaihe basin. Science of Soil and Water Conservation in China, 14(4): 50–59. (in Chinese)

Mann H B. 1945. Nonparametric test against trend. Econometrica, 13(3): 245–259.

Miao C Y, Sun Q H, Borthwick A G L, et al. 2016. Linkage between hourly precipitation events and atmospheric temperature changes over China during the Warm Season. Scientific Reports, 6: 22543, doi: 10.1038/srep22543.

Nilawar A P, Waikar M L. 2018. Impacts of climate change on streamflow and sediment concentration under RCP 4.5 and 8.5: A case study in Purna river basin, India. Science of the Total Environment, 650: 2685–2696.

Ouyang Z Y, Zheng H, Yue P. 2013. Establishment of ecological compensation mechanisms in China: Perspectives and strategies. Acta Ecologica Sinica, 33(3): 686–692. (in Chinese)

Petersen T, Devineni N, Sankarasubramanian A. 2012. Seasonality of monthly runoff over the continental United States: Causality and relations to mean annual and mean monthly distributions of moisture and energy. Journal of Hydrology, 468: 139–150.

Qiu D X, Wu C X, Mu X M, et al. 2022. Spatial-temporal analysis and prediction of precipitation extremes: A case study in the Weihe River Basin, China. Chinese Geographical Science, 32(2): 358–372.

Rodriguez-Iturbe I. 2000. Ecohydrology: A hydrologic perspective of climate-soil-vegetation dynamics. Water Resources Research, 36(1): 3–9.

Rossi M W, Whipple K X, Vivoni E R. 2016. Precipitation and evapotranspiration controls on daily runoff variability in the contiguous United States and Puerto Rico. Journal of Geophysical Research: Earth Surface, 121(1): 128–145.

Samain B, Pauwels V R N. 2013. Impact of potential and (scintillometer-based) actual evapotranspiration estimates on the performance of a lumped rainfall-runoff model. Hydrology and Earth System Sciences, 17(11): 4525–4540.

Shaanxi Province Department of Water Resources, 2019. Shaanxi Water Resources Bulletin. Xi'an: Shaanxi Province Department of Water Resources. (in Chinese)

Song J X, Xu Z X, Liu C M, et al. 2007. Ecological and environmental instream flow requirements for the Wei River—the

largest tributary of the Yellow River. Hydrological Processes, 21(8): 1066–1073.

Sun S L, Chen H S, Ju W M, et al. 2013. Effects of climate change on annual streamflow using climate elasticity in Poyang Lake Basin, China. Theoretical and Applied Climatology, 112(1–2): 169–183.

Sun Y X, Tang D S, Ding Y F, et al. 2016. A real-time operation of the Three Gorges Reservoir with flood risk analysis. Water Science and Technology Water Supply, 16(2): 551–562.

Vogel R M, Fennessey N M. 1994. Flow-duration curves. 2. New interpretation and confidence-intervals. Journal of Water Resources Planning and Management, 120(4): 485–504.

Walsh R P D, Lawler D M. 1981. Rainfall seasonality: Description, spatial patterns and change through time. Weather, 36: 201–208.

Wang X X, Su P, Lin Q D, et al. 2019. Distribution, assessment and coupling relationship of heavy metals and macroinvertebrates in sediments of the Weihe River Basin. Sustainable Cities and Society, 50: 101665, doi: 10.1016/j.scs.2019.101665.

Wen T F, Xiong L H, Jiang C, et al. 2019. Effects of climate variability and human activities on suspended sediment load in the Ganjiang River Basin, China. Journal of Hydrologic Engineering, 24(11): 05019029, doi: 10.1061/(ASCE)HE.1943-5584.0001859.

Wu C X, Qiu D X, Gao P, et al. 2022. Application of the InVEST model for assessing water yield and its response to precipitation and land use in the Weihe River Basin, China. Journal of Arid Land, 14(4): 426–440.

Xie X H, Liang S L, Yao Y J, et al. 2015. Detection and attribution of changes in hydrological cycle over the Three-North region of China: climate change versus afforestation effect. Agricultural and Forest Meteorology, 203: 74–87.

Xie Z B, Mu X M, Gao P, et al. 2022. Variation characteristics of runoff in the upper reaches of Beiluo River based on R/S and Morlet wavelet analysis. Research of Soil and Water Conservation, 29(2): 139–144. (in Chinese)

Yang H B, Qi J, Xu X Y, et al. 2014. The regional variation in climate elasticity and climate contribution to runoff across China. Journal of Hydrology, 517: 607–616.

Yang J, Jin J M, Shao J, et al. 2021. Vegetation restoration and its impact on runoff in typical areas of middle Loess Plateau. Transactions of the Chinese Society for Agricultural Machinery, 52(5): 258–266, 257. (in Chinese)

Yang L, Zhao G J, Tian P, et al. 2022. Runoff changes in the major river basins of China and their responses to potential driving forces. Journal of Hydrology, 607: 127536, doi: 10.1016/j.jhydrol.2022.127536.

Zeng L, Li J, Zhou Z X, et al. 2020. Optimizing land use patterns for the grain for Green Project based on the efficiency of ecosystem services under different objectives. Ecological Indicators, 114: 106347, doi: 10.1016/j.ecolind.2020.106347.

Zhan C S, Jiang S S, Sun F B, et al. 2014. Quantitative contribution of climate change and human activities to runoff changes in the Wei River basin, China. Hydrology and Earth System Sciences, 18(8): 3069–3077.

Zhang B Q, He C S. 2016. A modified water demand estimation method for drought identification over arid and semiarid regions. Agricultural and Forest Meteorology, 230: 58–66.

Zhang K, Lu Y H, Fu B J, et al. 2018. The effects of restoration on vegetation trends: spatiotemporal variability and influencing factors. Earth and Environmental Science Transactions of the Royal Society of Edinburgh, 109(3–4): 473–481.

Zhao G J, Mu X M, Tian P, et al. 2013. Climate changes and their impacts on water resources in semiarid regions: a case study of the Wei River basin, China. Hydrological Processes, 27(26): 3852–3863.

Zhou A K, Yan B W. 2014. Fractal characteristics of monthly runoff process in Wei River watershed. Journal of Hydroelectric Engineering, 33(4): 7–13. (in Chinese)

Zuo D P, Xu Z X, Zhao J, et al. 2015. Response of runoff to climate change in the Wei River basin, China. Hydrological Sciences Journal, 60(3): 508–522.